Supporting Information

Reversing the Dendrite Growth Direction and Eliminating Concentration Polarization via Internal Electric Field for Stable Lithium Metal Anodes

Yue Ma [a,c], Feng Wu [a,b,c], Nan Chen [a,b], Yitian Ma [a], Chao Yang [d], Yanxin Shang [a,c], Hanxiao Liu [a,c], Li Li [a,b,c], and Renjie Chen* [a,b,c]*

[a]Beijing Key Laboratory of Environmental Science and Engineering, School of Materials Science and Engineering, Beijing Institute of Technology, Beijing 100081, China

[b]Collaborative Innovation Center of Electric Vehicles in Beijing, Beijing 100081, China

[c]Advanced Technology Research Institute, Beijing Institute of Technology, Jinan 250300, China

[d]Helmholtz Zentrum Berlin Mat & Energie, D-14109 Berlin, Germany

*Corresponding Authors
Renjie Chen, E-mail: chenrj@bit.edu.cn
Nan Chen, E-mail: chenn@bit.edu.cn

Experimental Section

Materials

Au target (99.99%) was purchased from Zhongnuo Advanced Materials (Beijing) Technology Co., Ltd. The ether electrolyte composing of 1.0 M Lithium bis(trifluoromethanesulfonyl)imide (LiTFSI) and 1,3-dioxolane (DOL)/ dimethyl ether (DME) (v:v, 1:1) was configurated from DoDoChem. The ester electrolyte consisting of 1.0 M lithium hexafluorophosphate ($LiPF_6$) and ethylene carbonate (EC)/ diethyl carbonate (DEC)/ ethyl methyl carbonate (EMC) (v:v:v, 1:1:1) was configurated from DoDoChem. All regents were used without any purification.

Material synthesis

The separator (Celgard 2325, 25 μm thick) was loaded into DC magnetron sputtering system (JPG-450a, SKY Technology Development Co., Ltd) for coating using one Au target (99.99%). The manufacturing process was carried out at the condition as follows: sputtering power of 30 W, sputtering temperature of 25 °C, working pressure of 0.5 Pa and sputtering time of 30 seconds. The distance between target and substrate was set as 10 cm. The average loading mass of Au coated layer is about 0.02 mg cm^{-2}.

240 mg Lithium iron phosphate ($LiFePO_4$, LFP) or $LiNi_{0.8}Co_{0.1}Mn_{0.1}O_2$ (NCM811) particles, 30 mg Super-P and 30 mg PVDF were mixed in N-methylpyrrolidinone (NMP) and ball milled for 0.5 h to form uniform slurry. Then, the slurry was casted on the Al foil and then dried at 60 °C for one night under vacuum. The prepared electrode was pouched into pieces with diameter of 11.0 mm for assembling full cells. The mass loading of LFP and NCM811 cathodes are ~2.4 mg cm^{-2} and ~2.8 mg cm^{-2}, respectively.

Materials Characterizations

The DC magnetron sputtering system (JPG-450a, SKY Technology Development Co., Ltd) was operated to sputter the Au nanoparticles on the commercial separator. The contact angles of the ether electrolyte on the blank and Au-modified separator were measured using a contact angle analyzer

(OCA 25, Dataphysics, Germany). Scanning electron microscopy (SEM) photographs were obtained using a HITACHI S-3500N scanning electron microscope. Atomic Force Microscope (AFM) images were obtained using Buker Icon. The X-ray photoelectron spectroscopy testing was carried out using a spectrometer (PHI QUANTERA-II SXM), which was fitted with a monochromatic Al Kα X-ray source (1486.6 eV) for excitation. Synchrotron X-ray tomography was carried out at the BAMline at BESSY II.

Electrochemical measurements

Coin-type cells were employed and assembled in an argon-filled glove box with the oxygen and water contents both below 0.1 ppm. To assemble Li||Cu coin cell, Cu disk, Au modified or blank separator and Li foil were placed in the sandwich structure with electrolyte. The used electrolyte was composing of 1.0 M Lithium bis(trifluoromethanesulfonyl)imide (LiTFSI) and 1,3-dioxolane (DOL)/ dimethyl ether (DME) (v:v, 1:1). The symmetric Li||Li cion cell was assembled with the ester electrolyte, which consist of 1.0 M lithium hexafluorophosphate ($LiPF_6$) and ethylene carbonate (EC)/ diethyl carbonate (DEC)/ ethyl methyl carbonate (EMC) (v:v:v, 1:1:1), and the Au modified or blank separator between electrodes. The thickness of the lithium anode used is 1 mm, and the diameter is 7 mm. For the Li||LFP full cells, the as-prepared cathode, separator, and Li metal anode were placed in standard CR2025 type coin shells. The used electrolyte for Li||LFP and Li||NCM811 cells were 1.0 M $LiPF_6$ and EC/DEC/ EMC (v:v:v, 1:1:1). The thickness of the lithium anode used is 2 mm, and the diameter is 15.6 mm. Galvanostatic cycling was conducted on a Land Cell tester (CT2001A, Wuhan Jinnuo Company). Electrochemical impedance spectroscopy (EIS) measurements were performed on electrochemical workstation (CHI660E, Shanghai Chenhua Company). The method of calculating ionic conductivity of separator was based on EIS measurement of (stainless steel) SS||SS cells. Ionic conductivity of the separator can be calculated by using an equation:

$$\sigma = L/(R \cdot S)$$

where L is the thickness, R is the resistance, and S is the contact area of SS.

The lithium transfer number (tLi+) is measured by Li||Li cell with different separator, and the value is calculated as follows:

$$t_{Li^+} = \frac{I_s(\Delta V - I_0 R_0)}{I_0(\Delta V - I_s R_s)}$$

where R0 and Rs are the interfacial resistance before and after polarization, I_0 and I_s represent the current value in initial and steady under a polarization potential of 10 mV in the DC process, respectively.

Computational methods

We have employed the Vienna Ab Initio Package (VASP) [1,2] to perform all the density functional theory (DFT) calculations within the generalized gradient approximation (GGA) using the PBE [3] formulation. We have chosen the projected augmented wave (PAW) potentials [4,5] to describe the ionic cores and take valence electrons into account using a plane wave basis set with a kinetic energy cutoff of 450 eV. Partial occupancies of the Kohn−Sham orbitals were allowed using the Gaussian smearing method and a width of 0.05 eV. The electronic energy was considered self-consistent when the energy change was smaller than 10^{-6} eV. Monkhorst-Pack k-points of 2×2×1 was applied for all the surface calculations. During structural optimizations of the surface models, a 3 × 3 × 1 gamma-point centered k-point grid for the Brillouin zone was used and the top two layers were allowed to fully relax while the bottom atomic two layers were fixed. A geometry optimization was considered convergent when the force change was smaller than 0.03 eV/Å. Grimme's DFT-D3 methodology [6] was used to describe the dispersion interactions.

The adsorption energy (Eads) of adsorbate A was defined as

$$E_{ads} = E_{A/surf} - E_{surf} - E_{A(g)}$$

where $E_{A/surf}$, E_{surf} and $E_{A(g)}$ are the energy of adsorbate A adsorbed on the surface, the energy of clean surface, and the energy of isolated A molecule in a cubic periodic box, respectively.

COMSOL methods: FEM conducted by COMSOL Multiphysics has been used to investigate the distribution of Li ions through our structure. The migration of Li ions driven by electric field and

diffusion flow in both liquid phase (electrolytes) and solid phase was considered in these simplified simulations. Two physical models of electrostatic and transport of diluted species based on the partial differential equations listed below were coupled to conduct FEM simulation [7,8].

$$E = -\nabla V$$
$$J_i = -D_i \nabla c_i + z_i \mu_{m,i} F c_i E$$
$$\frac{\partial c_i}{\partial t} = -\nabla \bullet J_i$$

where E is the electric field (V), V is the electric potential (V), J_i is the flux vector of component i (mol m^{-2} s^{-1}), D_i is the diffusion coefficient of component i (m^2 s^{-1}), c_i is the concentration of component i (mol m^{-3}), z_i is the charge number of component i, $\mu_{m,i}$ is the ion mobility of component i (mol s kg^{-1}), F is the Faraday constant, and t is the diffusion time. These FEM simulations on the routine our composite separator was performed in a rectangle area, respectively. The potential difference ΔV through these electrolytes was set as 2.7-4.2 V. To investigate the ion transport behaviors with limited liquid electrolytes in long time cycling, the same physical model was established and the ratio of diffusion coefficients of Li ions in liquid electrolytes and solid particles was decreased to 10.0. The mobilities of Li ions m for liquid electrolyte and solid particles are defined by the Nernst-Einstein equation. The bottom boundaries of two simulation areas are the Dirichlet boundaries with V_0 = 2.7 V and c_0 = 0 M. The top boundaries of two simulation area are also Dirichlet boundaries with V_1 =4.2 V and c_1 = 1.0 M. The other boundaries are natural boundaries with zero flux. Phase field model has been used in our FEM simulations.

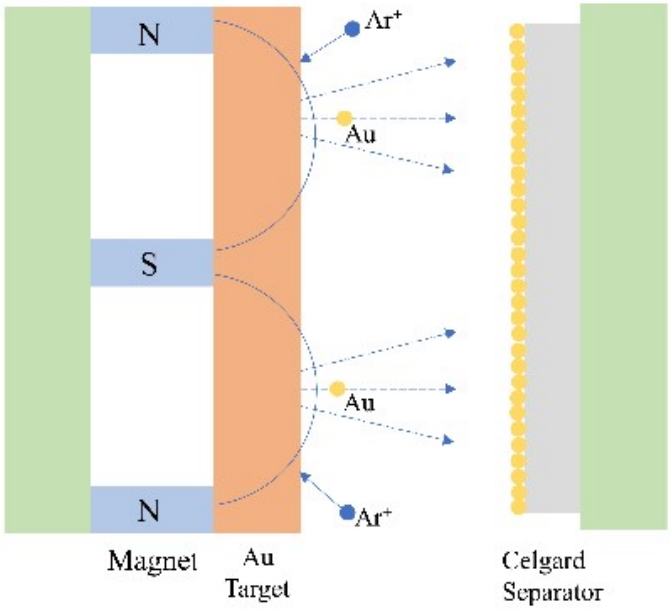

Figure S1. Schematic of the synthesis of Au-modified separator by a DC magnetron sputtering system.

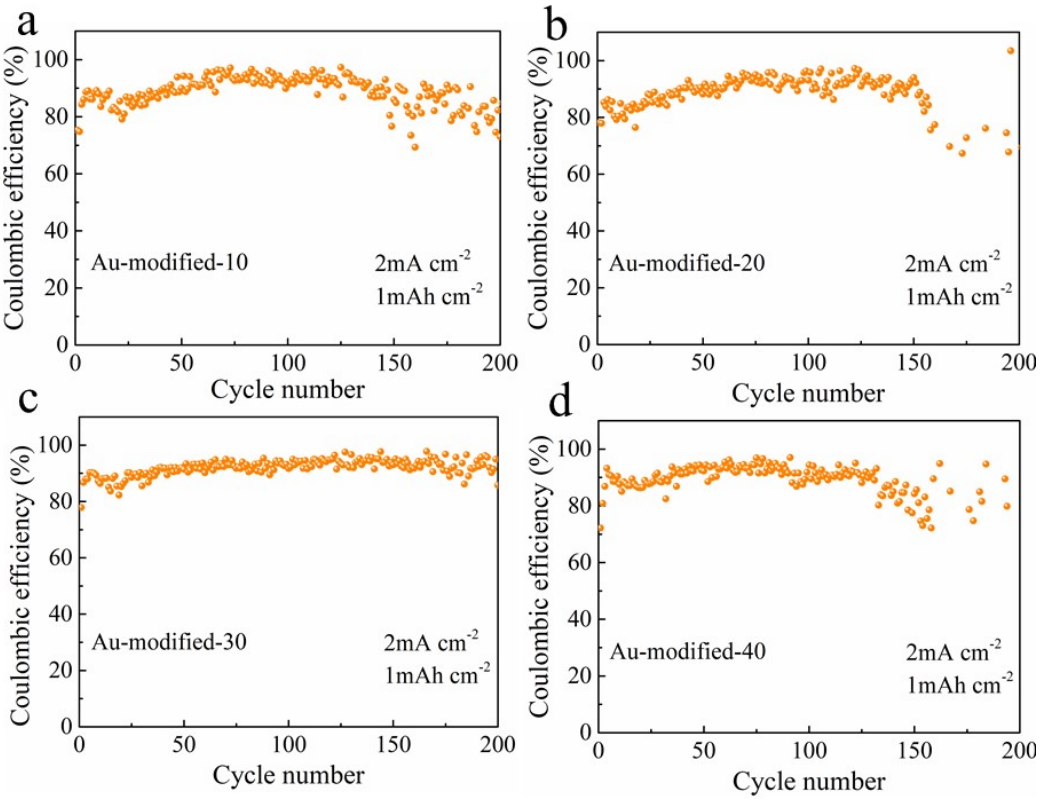

Figure S2. Coulombic efficiency of Li||Cu cells with Au-modified separators of different sputtering time.

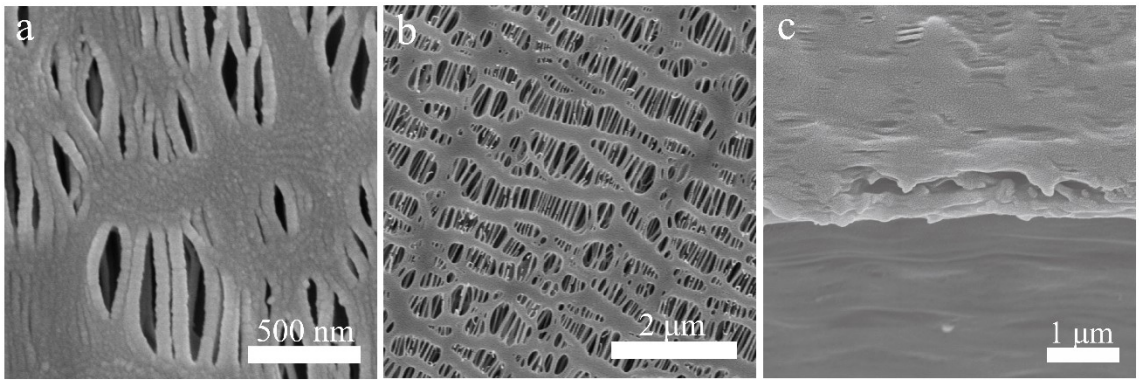

Figure S3. SEM images of the Au-modified separator. (a) Top view of back side and (b) Cross-section.

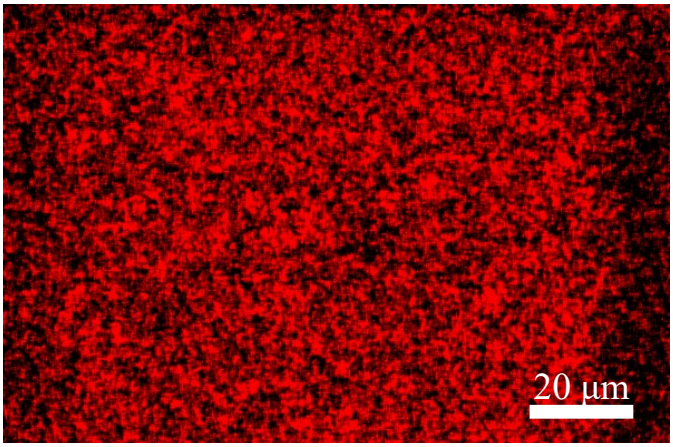

Figure S4. EDS mapping images of element C of Au-modified

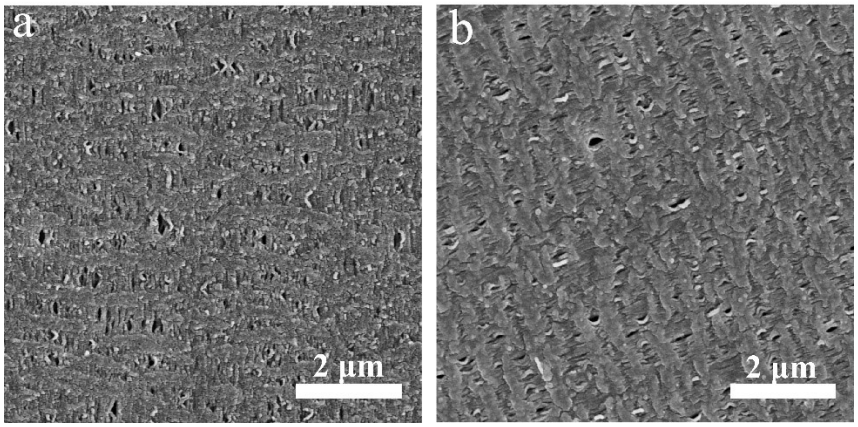

Figure S5. The SEM images of Au-modified separator of Li||Cu cells after 1 and 10 cycles.

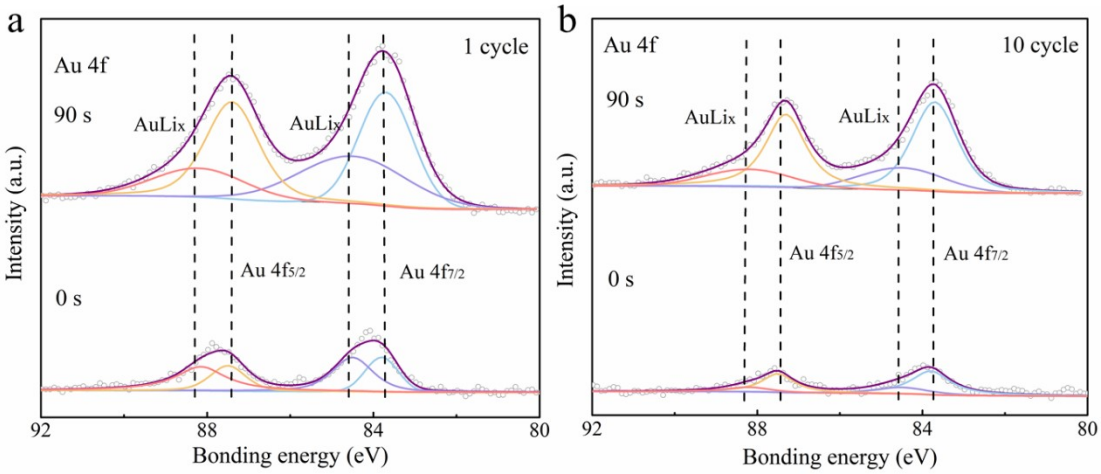

Figure S6. The depth XPS spectra of Au-modified separator of Li||Cu cells after 1 and 10 cycles.

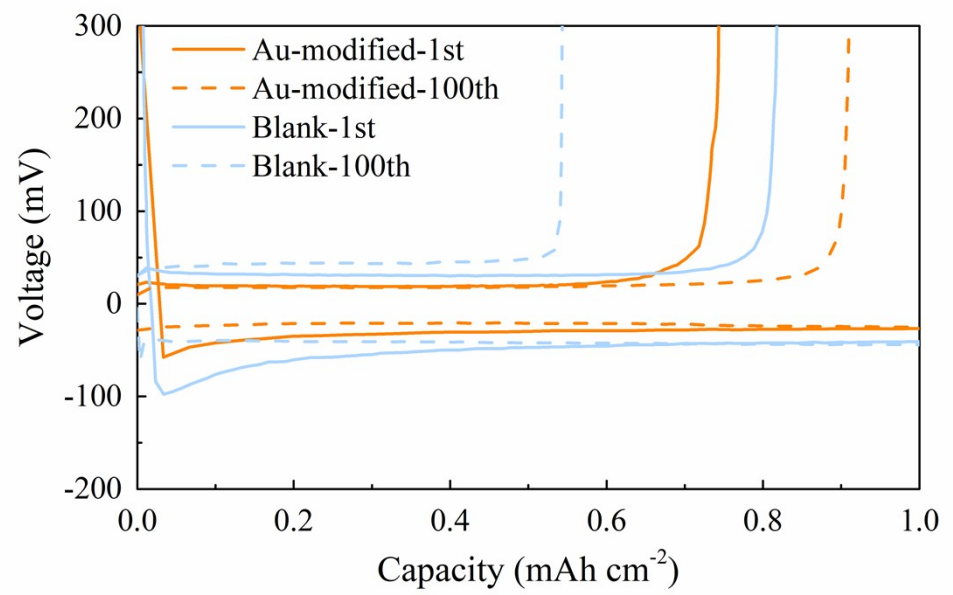

Figure S7. The voltage profiles of Li||Cu cells after 1 and 100 cycles.

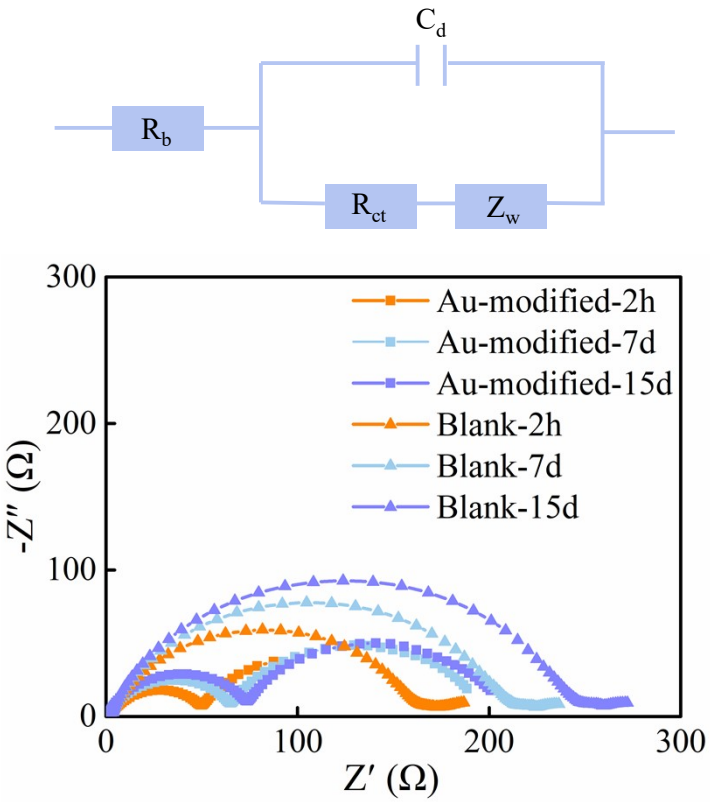

Figure S8. Static impedance of Li||Li cells at original state, 7 and 15 days rest.

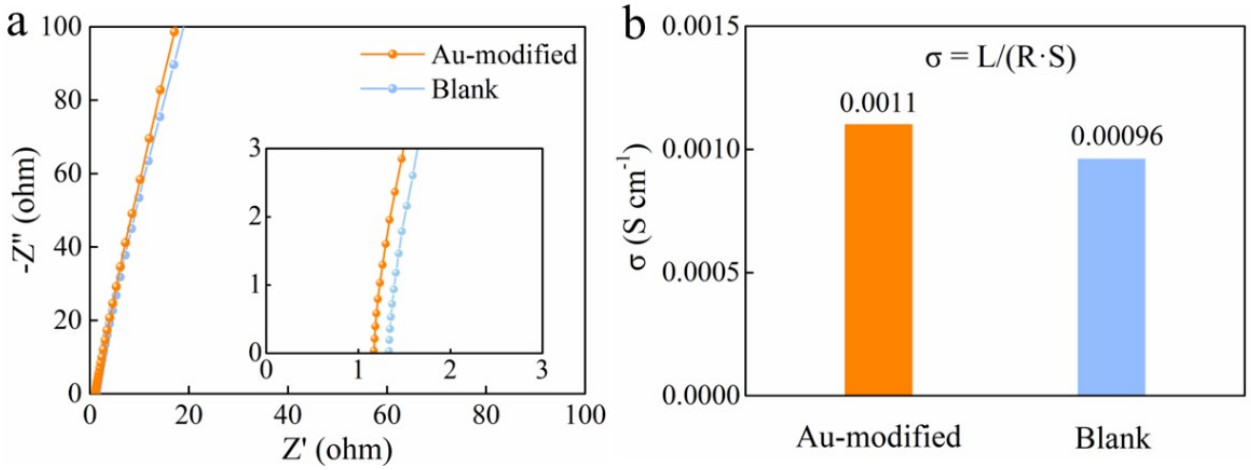

Figure S9 (a) Impedance plots of SS||SS cells and (b) the corresponding ionic conductivity of Au-modified and blank separators.

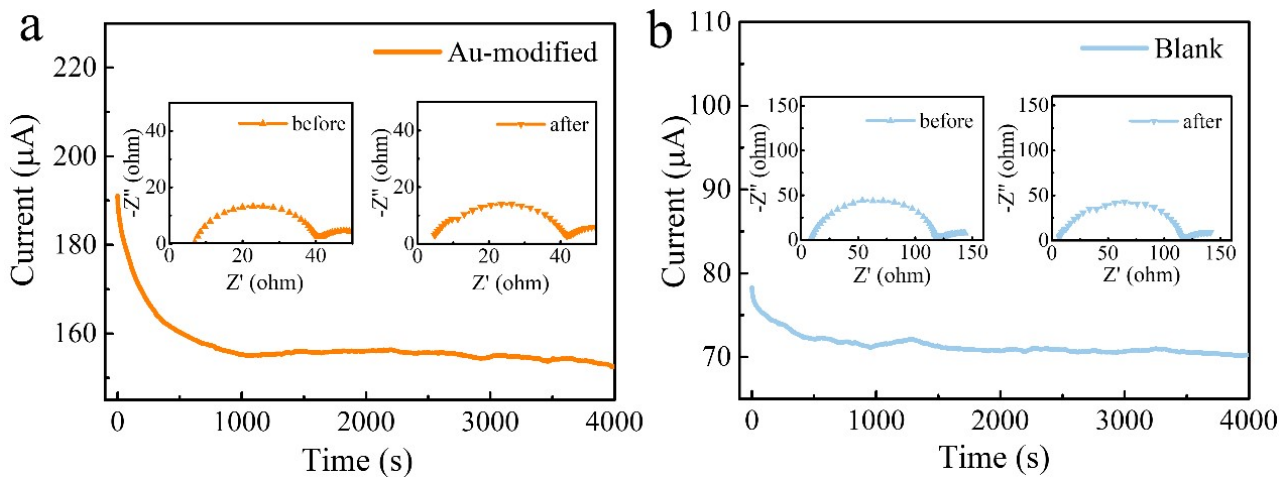

Fig. S10 Measurement of t_{Li+} using potential polarization of Li||Li symmetric cells with (a) Au-modified separator; (b) blank separator.

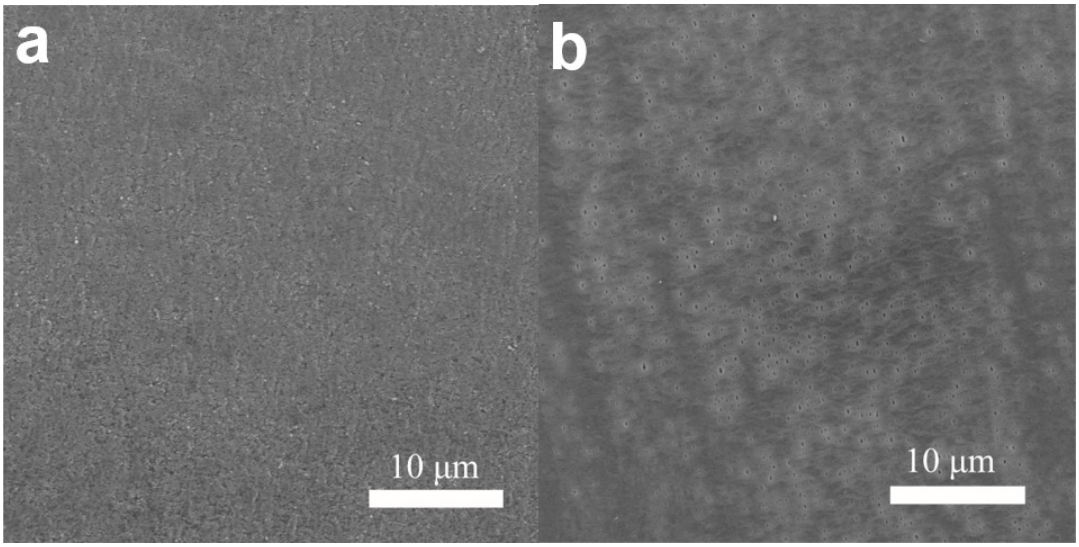

Figure S11. Top view SEM images of Li anode in the cells with Au-modified (a) and blank (b) separator after the 150th cycle.

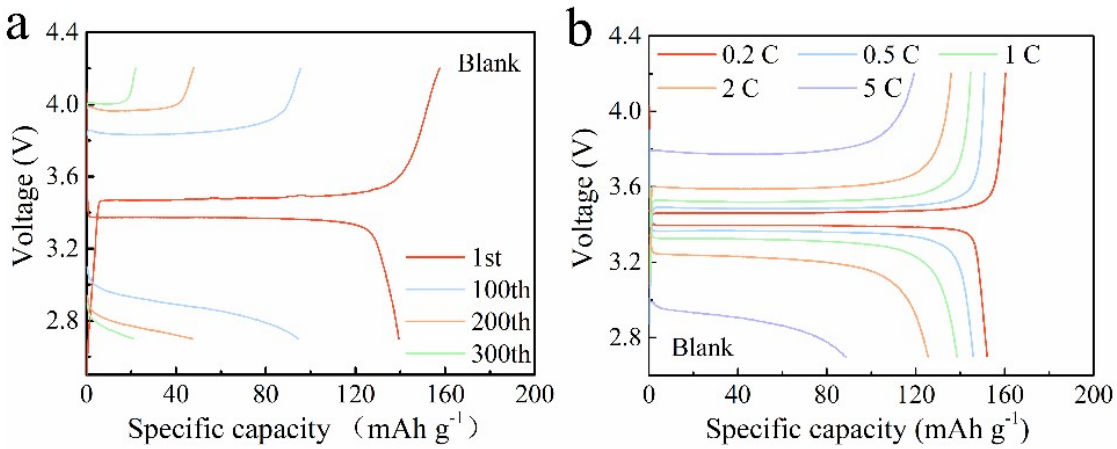

Figure S12. The voltage profiles of Li||LFP cell with blank separator at different cycles and rates.

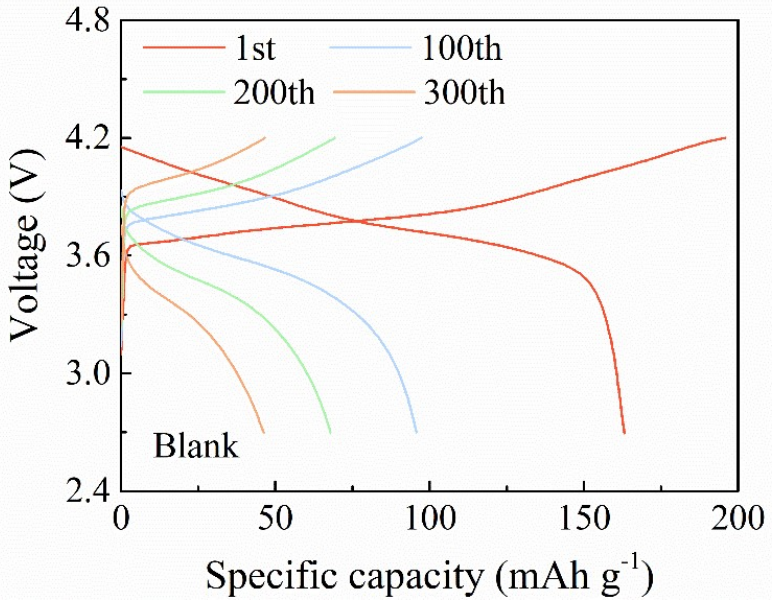

Figure S13. The corresponding voltage profiles of the Li||NCM811 cell with blank separator at different cycles.

Table S1. Compositions of full-cell cycling with different approaches to protect Li metal based on the ether electrolytes

Work	**Electrochemical Propertise**	**Ref**
n-terminal alcohols treated Li	NCM, 0.1C, 90 cycles, capacity retain >80%	9
Lithium-mont-morillonite SEI	LFP, 1C, 400 cycles, >90%	10
Li-Ag-LiF SEI	NCM333, 1C, 100 cycles, >75.8%	11
PVDF-HFP-LiF layer	LFP, 0.5C, 250 cycles, >80%	12
N-organic/Li_3N@Li	NCM622, 1C, 100 cycles, >99%	13
Au-modified separaotr	LFP, 1C, 350 cycles, >97.8% NCM811, 1C, 300 cycles, >75.1%	**This work**

References

1 G. Kresse, J. Furthmüller, Comput. Mater. Sci., 1996, **6**, 15.

2 G. Kresse, J. Furthmüller, Phys. Rev. B., 1996, **54**, 11169.

3 J. P. Perdew, K. Burke, M. Ernzerhof, Phys. Rev. Lett., 1996, **77**, 3865.

4 G. Kresse, D. Joubert, Phys. Rev. B., 1999, **59**, 1758.

5 P. E. Blöchl, Phys. Rev. B., 1994, **50**, 17953-17979.

6 S. Grimme, J. Antony, S. Ehrlich, H. J. Krieg, J. Chem. Phys., 2010, **132**, 154104.

7 J. Newman, K.E. Thomas, H. Hafezi, D.R. Wheeler, Modeling of lithium-ion batteries, J. Power Sources., 2003, **119**, 838-843.

8 J. Newman, K.E. Thomas-Alyea, Prentice Hall, 2004.

9 D. Kang, N. Hart, J. Koh, L. Ma, W. Liang, J. Xu, S. Sardar, J. Lemmon. *Energy Stor. Mater.,* 2020, **24**, 618.

10 Y. Nan, S. Li, C. Han, H. Yan, Y. Ma, J. Liu, S. Yang, and B. Li. *Adv. Funct. Mater*., 2021, **31**, 2102336.

11 Z. Peng, J. Song, L. Huai, H. Jia, B. Xiao, L. Zou, G. Zhu, A. Martinez, S. Roy, V. Murugesan, H. Lee, X. Ren, Q. Li, D. Wang, W. Xu, and J. Zhang. *Adv. Energy Mater*., 2019, 1901764.

12 R. Xu, X. Zhang, X. Cheng, H. Peng, C. Zhao, C. Yan, and J. Huang. *Adv. Funct. Mater*., 2018, **28**, 1705838.

13 S. Ye, L. Wang, F. Liu, P. Shi, H. Wang, X. Wu, and Y. Yu. *Adv. Energy Mater*., 2020, 2002647.